



HAL
open science

Non-equilibrium turbulent boundary layers in high reynolds number flow at incompressible conditions: effects of streamline curvature and three dimensionality

Todd Lowe, Alexander J Smits, Michel Visonneau, Ganbo Deng, Liuyang Ding, Emmanuel Guilmineau, Richard Sandberg, Ali Haghiri, Aldo Gargiulo, Julie Duetsch-Patel, et al.

► To cite this version:

Todd Lowe, Alexander J Smits, Michel Visonneau, Ganbo Deng, Liuyang Ding, et al.. Non-equilibrium turbulent boundary layers in high reynolds number flow at incompressible conditions: effects of streamline curvature and three dimensionality. *Journal of Turbulence*, 2024, Non-equilibrium boundary layers, 25 (10-11), pp.386-398. 10.1080/14685248.2024.2395307 . hal-04785923

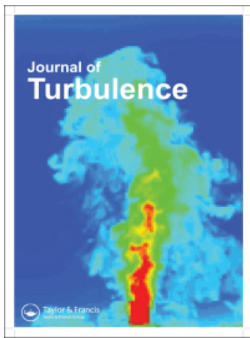
HAL Id: hal-04785923

<https://hal.science/hal-04785923v1>

Submitted on 19 Nov 2024

HAL is a multi-disciplinary open access archive for the deposit and dissemination of scientific research documents, whether they are published or not. The documents may come from teaching and research institutions in France or abroad, or from public or private research centers.

L'archive ouverte pluridisciplinaire **HAL**, est destinée au dépôt et à la diffusion de documents scientifiques de niveau recherche, publiés ou non, émanant des établissements d'enseignement et de recherche français ou étrangers, des laboratoires publics ou privés.



Non-equilibrium turbulent boundary layers in high reynolds number flow at incompressible conditions: effects of streamline curvature and three dimensionality

Todd Lowe, Alexander J. Smits, Michel Visonneau, Ganbo Deng, Liuyang Ding, Emmanuel Guilmineau, Richard Sandberg, Ali Haghiri, Aldo Gargiulo, Julie Duetsch-Patel, Philippe Lavoie, Daniel MacGregor, Luca Savio, Yngve L. Jenssen, Christopher Roy, Owen Williams, Serge Toxopeus & William Devenport

To cite this article: Todd Lowe, Alexander J. Smits, Michel Visonneau, Ganbo Deng, Liuyang Ding, Emmanuel Guilmineau, Richard Sandberg, Ali Haghiri, Aldo Gargiulo, Julie Duetsch-Patel, Philippe Lavoie, Daniel MacGregor, Luca Savio, Yngve L. Jenssen, Christopher Roy, Owen Williams, Serge Toxopeus & William Devenport (2024) Non-equilibrium turbulent boundary layers in high reynolds number flow at incompressible conditions: effects of streamline curvature and three dimensionality, Journal of Turbulence, 25:10-11, 386-398, DOI: [10.1080/14685248.2024.2395307](https://doi.org/10.1080/14685248.2024.2395307)

To link to this article: <https://doi.org/10.1080/14685248.2024.2395307>



© 2024 The Author(s). Published by Informa UK Limited, trading as Taylor & Francis Group



[View supplementary material](#)



Published online: 28 Aug 2024.



[Submit your article to this journal](#)



Article views: 447



[View related articles](#)













[View Crossmark data](#)



Citing articles: 1 [View citing articles](#)

Non-equilibrium turbulent boundary layers in high reynolds number flow at incompressible conditions: effects of streamline curvature and three dimensionality

Todd Lowe ^a, Alexander J. Smits ^b, Michel Visonneau ^c, Ganbo Deng ^c, Liuyang Ding^b, Emmanuel Guilmineau ^c, Richard Sandberg ^d, Ali Haghiri^{d,e}, Aldo Gargiulo^{a,f}, Julie Duetsch-Patel ^a, Philippe Lavoie ^g, Daniel MacGregor^g, Luca Savio ^{h,i}, Yngve L. Jenssen^h, Christopher Roy^a, Owen Williams^j, Serge Toxopeus^k and William Devenport ^a

^aVirginia Tech, Blacksburg, VA, USA; ^bPrinceton University, Princeton, NJ, US; ^cCNRS, LHEEA Lab. (ECN/CNRS), Nantes, France; ^dUniversity of Melbourne, Melbourne, Australia; ^eUniversity of Leicester, Leicester, UK; ^fUniversity of Virginia, Charlottesville, VA, US; ^gUniversity of Toronto Institute for Aerospace Studies (UTIAS), Toronto, ON, Canada; ^hSINTEF Ocean, Trondheim, Norway; ⁱNorwegian University of Science and Technology (NTNU), Trondheim, Norway; ^jUniversity of Washington, Seattle, WA, US; ^kMaritime Research Institute Netherlands (MARIN), Wageningen, The Netherlands

ABSTRACT

The physics and computational prediction of turbulent boundary layer flow over axisymmetric and three-dimensional bodies are examined. Three cases were considered for which extensive experimental results and companion Reynolds-averaged Navier Stokes (RANS) solutions were obtained and/or available in the open literature. These cases all have Reynolds numbers based upon the freestream velocity and body geometric scale on the order of 10^5 to 10^6 , which is large for laboratory scales but small compared to the maximum scales observed for full-scale vehicles. Despite significant differences in approach flow fields and geometries for these three cases, some common themes emerged in the findings. All cases involved complications due to pressure gradients combined with streamline curvature, and all exhibited regions of turbulence reduction due to accelerated flow. These complications led to discrepancies in computed results even in attached flow regions where it is often assumed that RANS models provide reliable predictions. The authors recommend further work on modelling approaches that can capture rapid distortion effects on turbulence transport that can be incorporated into industry-useful frameworks. Two cases involving laterally symmetric, three-dimensional wall-mounted hills with aft-body separation revealed that asymmetric mean flow fields are likely to result. This finding has been observed in experiments conducted in multiple facilities and in computations using multiple solvers and turbulence models. It is concluded that non-unique and asymmetric global flow solutions are fundamental to flow cases with lateral geometric symmetry involving turbulent boundary layer separation. Further work is also needed to accurately predict low-frequency unsteadiness due to geometries that produce non-unique mean flow fields. For such flows, it remains to be definitively determined whether experimentally observed modes of the mean flow are equivalent, or nearly equivalent, to asymmetric mean flow solutions obtained using RANS approaches.

ARTICLE HISTORY

Received 9 May 2024
Accepted 14 August 2024


KEYWORDS

Turbulent boundary layers; turbulence modelling; validation; symmetry breaking

1. Introduction

All aero/hydrodynamic flows of engineering relevance feature some degree of mean flow three-dimensionality and curvature of mean flow streamlines. These complications bring about a variety of challenges to the prediction, and even the physical understanding, of flows over three-dimensional bodies: relaminarization, symmetry breaking, very low-frequency unsteadiness, inflow profile sensitivity, embedded layers, flow skewing, convolution of pressure gradient/curvature effects, and three-dimensional separation of the boundary layer. Through the NATO AVT-349 activity, Non-Equilibrium Turbulent Boundary Layers in High Reynolds Number Flow at Incompressible Conditions, the Princeton Body of Revolution (BOR) [1] case and the hill case

CONTACT Todd Lowe  kelowe@vt.edu

 Supplemental data for this article can be accessed online at <https://doi.org/10.1080/14685248.2024.2395307>.

© 2024 The Author(s). Published by Informa UK Limited, trading as Taylor & Francis Group
This is an Open Access article distributed under the terms of the Creative Commons Attribution License (<http://creativecommons.org/licenses/by/4.0/>), which permits unrestricted use, distribution, and reproduction in any medium, provided the original work is properly cited. The terms on which this article has been published allow the posting of the Accepted Manuscript in a repository by the author(s) or with their consent.

from the Benchmark Validation Experiments for RANS/LES Investigations (BeVERLI) project [2] (hereafter referred to as the BeVERLI Hill) were supplemented with findings from the Gaussian hill case [3], referred to in the literature as the Boeing ‘speed-bump’ (BB), to explore the physics of, and our contemporary ability to model, these flows. This article provides our consensus position on the state of modelling for moderate and high Reynolds number flow over curved bodies along with the current needs for research that could significantly advance the field.

Instrumental to the work of NATO AVT-349 was the tight integration of experimental and numerical efforts. This was done to ensure close matching between boundary conditions found in both experiments and simulations. It also helped ensure that the appropriate data were gathered in the experiments to support and validate the modelling efforts. Where possible, cross-facility testing was performed to help quantify the impact of nominally small differences in test case conditions between facilities, strengthening the confidence in conclusions.

Each of the cases studied were shown to pose challenges for RANS computations and modelling. And while the well known challenges of prediction of smooth body turbulent separation are present in both the BeVERLI Hill and the BB cases, modelling differences were present in attached regions of flow as well, including the BOR experiment which does not exhibit boundary layer separation. The complications that appear to be most responsible for these differences are the turbulence reduction and redistribution effects of large accelerations, the convolved effects of pressure gradient and curvature, and mean flow non-uniqueness.

After briefly describing each of the three flow cases studied, the remainder of the article focuses on our findings and recommendations. Extensive supporting information on the cases is provided in appendices.

2. Flow cases

2.1. Body of revolution

Here, we examine the case where a body-of-revolution is placed on the centreline of a fully-developed turbulent pipe flow, thereby imposing on the turbulence the effects of pressure gradient, streamline curvature, and flow divergence. The case includes the far-wake where the turbulence relaxes to its equilibrium conditions, albeit very slowly.

Figure 1 illustrates the test configuration. The body consisted of three parts – the bow section ($0 < x/R < 2.67$), the cylindrical recovery section ($2.67 < x/R < 10$), and the stern section ($10 < x/R < 12.67$). The bow section is a half prolate spheroid, the recovery section has a constant diameter d , and the contour of the stern follows a 4th-order power law to minimise the drag [4]. The presence of the body causes the incoming turbulent pipe flow to experience a favourable pressure gradient (FPG), streamline divergence and convex curvature over the bow, followed by a relaxation over the recovery section, and an adverse pressure gradient (APG), streamline convergence, and convex curvature over the stern region. Far downstream the flow then slowly recovers to its initial state. Three body diameters were experimentally studied, only the results from the case of $d/D = \sqrt{2}/3$ are compared to computations in the current work.

The experiments and computations were previously reported by Ding et al. [1] and Visonneau et al. [5]. While briefly introduced here, key supporting experimental and computational results are available in Appendix A.

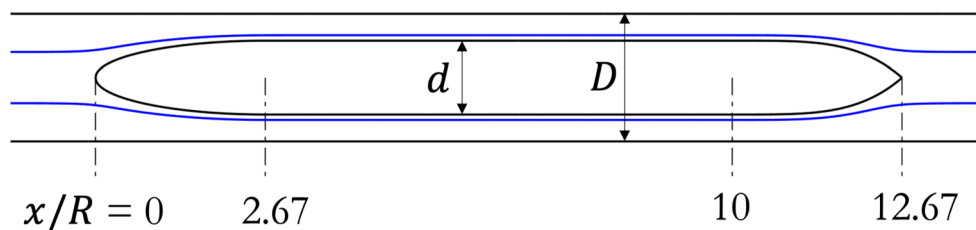


Figure 1. Test section geometry. The results in the current work are for $d/D = \sqrt{2}/3$. Blue solid lines are selected streamlines from a potential flow calculation. Flow is from left to right.

In the experiments, a streamlined axisymmetric body was placed on the centreline of a long pipe that has an inner diameter of $D = 2R = 38.1$ mm. The body was rigidly supported by an aerodynamically shaped sting (NACA 0015) (more detail of the set-up is given in [1]). The inflow was ensured to be fully-developed turbulent pipe flow by allowing $200D$ of development length upstream of the body. The bulk velocity U_b was ≈ 4.1 m/s, corresponding to $Re_D = U_b D / \nu \approx 156,000$, where $\nu = 10^{-6}$ m²/s is the kinematic viscosity of water at 20°C. Using the friction factor correlation reported by McKeon et al. [6], the upstream friction velocity was determined to be $u_\tau = 0.186$ m/s, and $Re_\tau = u_\tau R / \nu = 3550$. The experiment leveraged particle-image velocimetry (PIV) measurements to characterise the mean flow and turbulence in the bow and mid-body regions. The reliability of the measurements was assessed by comparison to past measurements and direct numerical simulation (DNS) at similar Reynolds numbers.

Reynolds-averaged Navier Stokes (RANS) computations were performed by groups from École Centrale de Nantes – Centre National de la Recherche Scientifique (CNRS) and the University of Melbourne. The work at CNRS used two turbulence models: the linear isotropic $k-\omega$ SST model by Menter [7] and a Reynolds stress transport model based on the SSG-LRR pressure-strain model [8]. The University of Melbourne computations were performed using the 2003 Menter $k-\omega$ Shear Stress Transport two-equation eddy-viscosity model [9, 10] as baseline and compared to results from a data-driven model based on the Gene-Expression Programming (GEP) [11] framework, the latter adopting both GEP ‘frozen’ and ‘CFD-driven’ approaches [12]. For the ‘frozen’ campaign of simulations, model development was purposely not based on the BOR experimental data available but rather on different configurations with similar characteristics (wall-mounted square cylinder, jet flows, airfoil) to assess generalizability of such models. As for the ‘CFD-driven’ approach, several models were developed using distinct cost functions, in particular exploiting recent multi-objective capability of the GEP framework [13]. GEP-based models were trained to learn a non-linear explicit algebraic Reynolds stress tensor ($\hat{\sigma}_{ij}^{x, GEP}$), and also a turbulent-kinetic-energy-corrective term (\hat{R}_{ij}^{GEP}), as proposed by Schmelzer et al. [14]. The explicit expressions of the best performing GEP models are given in Appendix B.

2.2. BeVERLI hill

The Benchmark Validation Experiment for RANS/LES Investigations (BeVERLI) aims to examine the evolution of an initially planar turbulent boundary layer (TBL) within an incompressible, high Reynolds number flow over a three-dimensional (3D) hill with a smooth surface, formally designated as the BeVERLI Hill. This geometric configuration is carefully designed to expose the flow to a diverse spectrum of physics akin to the aerodynamics experienced by high-lift devices, including varying degrees of separation and non-equilibrium effects induced by the concurrent action of spatially varying pressure gradients and streamline curvature.

The BeVERLI Hill geometry is depicted in Figure 2. The hill is characterised by a design length, w , measuring 0.9347 m, and a height, H , measuring 0.1869 m. The aspect ratio, w/H , is thus 5. A Cartesian coordinate system, x_i , is utilised to define this geometry. Specifically, the base of the hill is situated in the x_1 - x_3 plane, while its height extends in the x_2 direction. The geometry has been fully described by Gargiulo et al. [15]; and a 3D computer model of the BeVERLI Hill, accurately defining the lofted corners, was created using SolidWorks 3D CAD software and is available for download at <https://roy.aoe.vt.edu/vt-nasa-validation-challenge>.

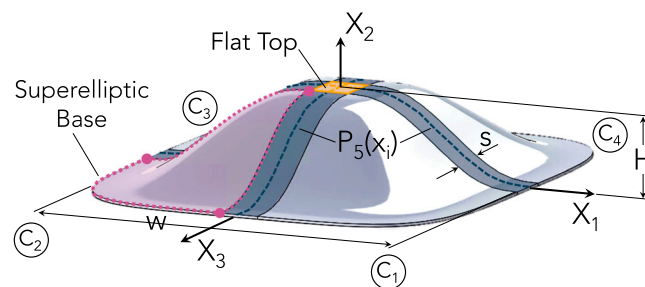


Figure 2. The BeVERLI Hill geometry. Polynomials (blue dashed lines); lines joining polynomials (yellow dashed lines); cylindrical sections (blue shaded surfaces); flat top (yellow shaded surface). Corner C_2 (mulberry shaded surface) is highlighted, along with its three constraining edges (dotted mulberry lines). This figure was originally reproduced by Gargiulo et al. [2].

Experiments on this case have been conducted at Virginia Tech [2, 16], the University of Toronto Institute for Aerospace Studies (UTIAS), and SINTEF Ocean [17]. The focus Reynolds numbers, based on hill height, for this study are $Re_H = 250,000$ and $650,000$, while the hill height, H , to boundary layer thickness, δ ratio is $H/\delta \approx 3$. Results have been obtained using a wide range of instruments and techniques, including surface steady [2, 17] and unsteady [18] pressure, particle-image velocimetry [15, 19], laser-Doppler velocimetry [16, 20, 21], oil-film interferometry [22], unsteady force transducers [17], and oil-flow visualisation [23]. Geometrically similar configurations have been tested in three different facilities at matched or nearly matched Reynolds numbers, and major results are consistent. Notably, all facilities have documented the presence of mean-flow asymmetry for laterally symmetric BeVERLI Hill configurations.

For the cases documented herein, RANS computations have been performed at Virginia Tech, the University of Melbourne, and École Centrale de Nantes - Centre National de la Recherche Scientifique. One- and two-equation linear and nonlinear eddy viscosity models, Reynolds stress transport models, and data-driven models have been used in these studies. Results from the computations and their comparisons to experiments are provided in detail in Appendix C.

2.3. Boeing Gaussian speed-bump

The Boeing Gaussian speed-bump (BB) case was developed by a team at Boeing and explored initially in experiments at the University of Washington [3], followed by Notre Dame [24]. This case was designed to have contrasting characteristics with some of the previous hills and bumps in the literature and to be less three-dimensional along the centreline. Its definition encompasses the hill geometry, the inflow boundary layer on a splitter plate, and the surrounding confinement of tunnel walls. It comprises a hill mounted to a flat plate that is Gaussian in the streamwise direction and incorporates an error function shaped shoulder profile to minimise complicated interactions toward the side walls. A comparison between the shapes of the BB and other hills is shown in Figure 3. The BB is designed to have a relatively thin boundary layer relative to the hill itself ($H/\delta = 10 - 12$, where H is the bump height) in an effort to be more relevant to wing-type applications. This is almost an order magnitude thinner than the BeVERLI Hill and most other axisymmetric hills that have been studied [25]. As a result, the curvature influence (R/δ) on the shear layers is relatively weaker compared to that of pressure gradients.

Experiments on this geometry have been conducted at the University of Washington and the University of Notre Dame [3, 24, 27–29], highlighting not only the three-dimensional topology of this configuration, but also large-scale flowfield features, turbulent stresses and surface pressures.

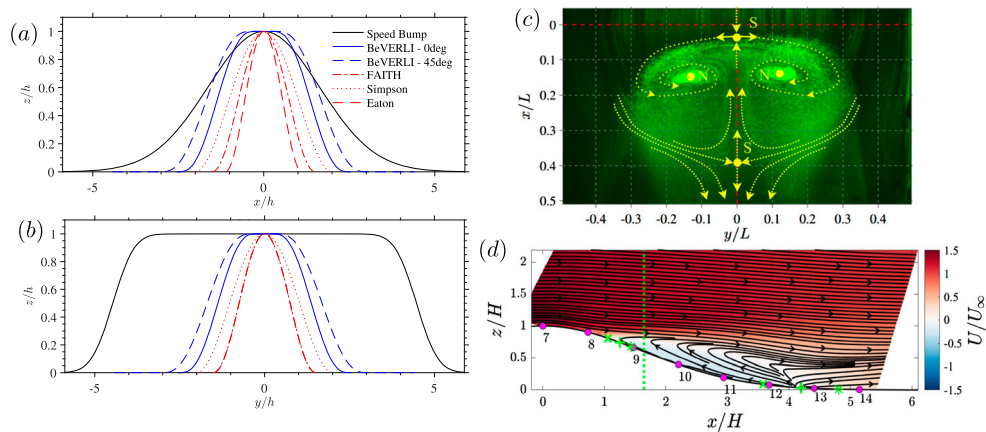


Figure 3. Comparison of the BB and other hill-type geometries in the (a) streamwise and (b) spanwise directions. All dimensions relative to maximum hill height, H . (c) Surface flow visualisation of the BB separation topology resembling an owl-type pattern of the first kind (adapted from [3]). (d) Centerline flowfield in the wake of the bump from PIV suggesting that the downstream saddle point is not a mean reattachment point, consistent with the owl-type pattern. Green dashed lines indicate the location of the change in sign of the surface curvature and pink dots indicate the location of pressure taps (from [26]).

A wide range of simulations have also been conducted including RANS [24, 27, 28], wall-modelled large-eddy simulation (WMLES) [30–32], wall-resolved large-eddy simulation (WRLES) [33, 34], and DNS [35–37], among others.

Further details of the experiments and computations focussed on the BB case are provided in Appendix E.

3. Relaminarization

Although Reynolds number dependent and accentuated at lower Reynolds numbers, the values of acceleration parameter ($K = \nu/U_e^2(\partial U_e/\partial s)$, where ν is the kinematic viscosity, U_e is the boundary layer edge velocity, and s is a curvilinear coordinate following the boundary layer edge streamline) on windward faces for both the BeVERLI Hill and BB cases indicate that they lie on the spectrum of relaminarizing flows (e.g., see [30, 35, 38]). The potential extremity of the phenomenon is highlighted by observations that occur for the 0° incidence BeVERLI Hill case and the BB at low Reynolds number: both have shown a laminar separation bubble forming just downstream of the suction peak which disappears at sufficient Reynolds number (e.g., [23]). The results for the Princeton BOR also indicate that the windward portion of this flow exhibits relaminarization-like turbulence reduction. In the case of the BB, the identification of this phenomenon has confirmed hypotheses from experiments [3] for the source of unexpected Reynolds number dependence of the separation bubble (seen to grow with Reynolds number). Many RANS or WMLES cases predict little to no separation under these conditions [30–32, 35]. This may be due to increases in predicted turbulent kinetic energy just downstream of accelerated flow regions as it enters the adverse pressure gradient region, resisting separation. Evidence of differences between experimental data and RANS solutions are seen also in the Princeton BOR case and the BeVERLI Hill. The mean velocity and Reynolds shear stress profiles in the bow region of the BOR (e.g. Figure 4), show dramatic differences that develop over the accelerating region. This is turbulence model dependent, with improvements shown for Reynolds stress models (Figure 4) and gene expression programming-based models (Figure 5). For the BeVERLI Hill case there is modelling dependency of pressure coefficient values around, and downstream of, the suction peak (see Figures 6–8), indicative of accrued deviations in Reynolds stress effects prior to encountering the adverse pressure gradient at the top of the hill. Results similar to these were shown in computational results from a wide group of contributors employing varying turbulence models and solvers for a blind validation challenge conducted using the BeVERLI Hill configuration with an asymmetric lateral geometry with a 30° yaw angle relative to the most bluff symmetric configuration [39–41]. These recent results show that all RANS-based solutions overpredict the magnitude of the suction peak at the top of the BeVERLI Hill, while offering some early evidence that scale-resolving methods may improve suction peak predictions. More substantial evidence for improving calculations with scale resolving approaches have been provided for the BB case [30, 35], although some wall-modelled large eddy simulations (WMLES) still failed to fully capture relaminarization effects, resulting in overprediction of turbulent kinetic energy levels at the top of the BB and subsequently the incorrect prediction of little or no separation [30–32, 35]. Advancing RANS modelling for acceleration-related turbulence reduction will be difficult and will likely require attention to ensuring that rapid distortion pressure-diffusion terms provide sufficient reductions in the turbulence transport [42]. (See also chapter 5 in [21] for experimental evidence of this need.) More likely scale-resolving approaches are needed to capture key phenomena sufficiently to obtain accurate forebody and suction peak pressure predictions. For instance, in addition to turbulence reduction due to acceleration, outer layer turbulent eddies that are remnants of the approach boundary layer will cause meandering of the suction pressure peak that will not be captured by steady RANS. Hybrid scale-resolving approaches like improved delayed-detached eddy simulation (IDDES) [43] may be a reasonable compromise for better capturing relaminarization and mean flow meandering when computational resources cannot support wall resolved or wall-modelled large-eddy simulation (e.g.see IDDES data for BeVERLI Hill in [40]).

Further complicating the modelling of the critical forebody flow region is the additional convolved effect of longitudinal curvature. The resulting variation of pressure normal to the wall requires considerations for modelling, and isolating the precise effects to the expression of turbulent stresses on the flow field is difficult. Additional explorations are needed that can decouple the effects of pressure gradient and curvature or that provide ranges of parameters and a reduced-order modelling approach to deconvolve the effects. Furthermore, the BeVERLI Hill case at 45° is likely to have effects due to lateral convex curvature near the centreline

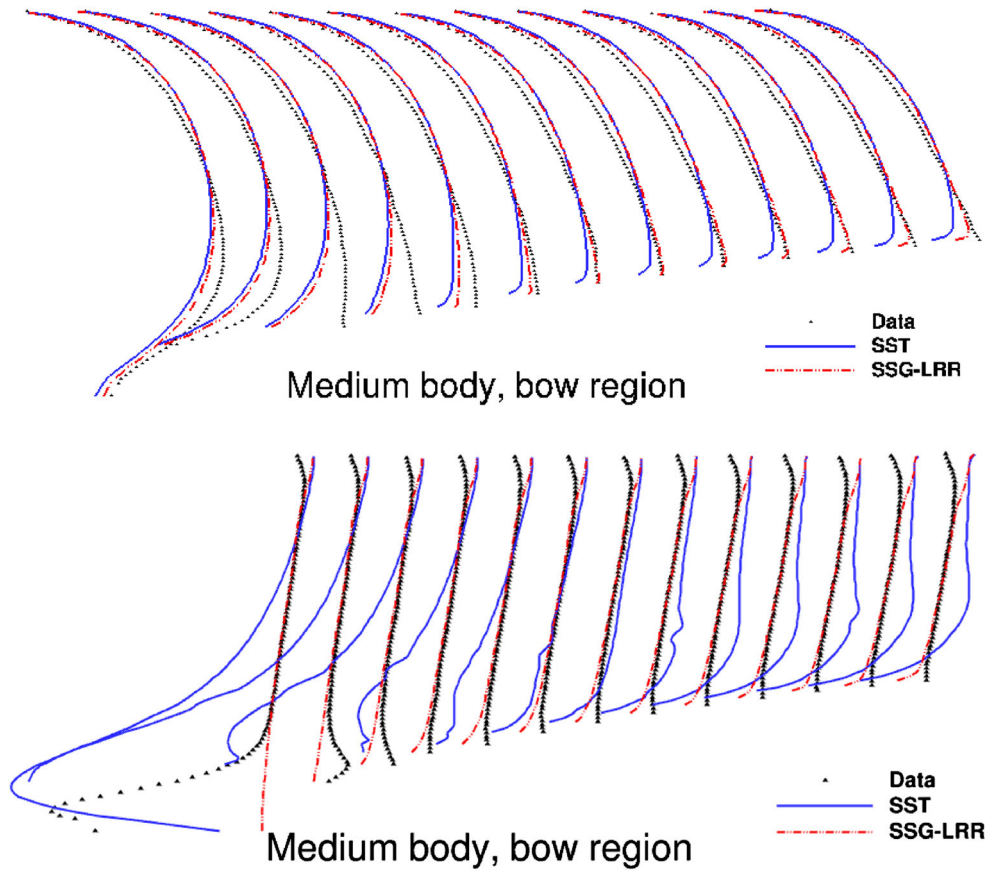


Figure 4. Bow region. Top: axial velocity profiles. Bottom: shear stress profiles. Profiles are shown from $x/R = -0.1$ to $x/R = 1.1$ with a $0.1R$ increment.

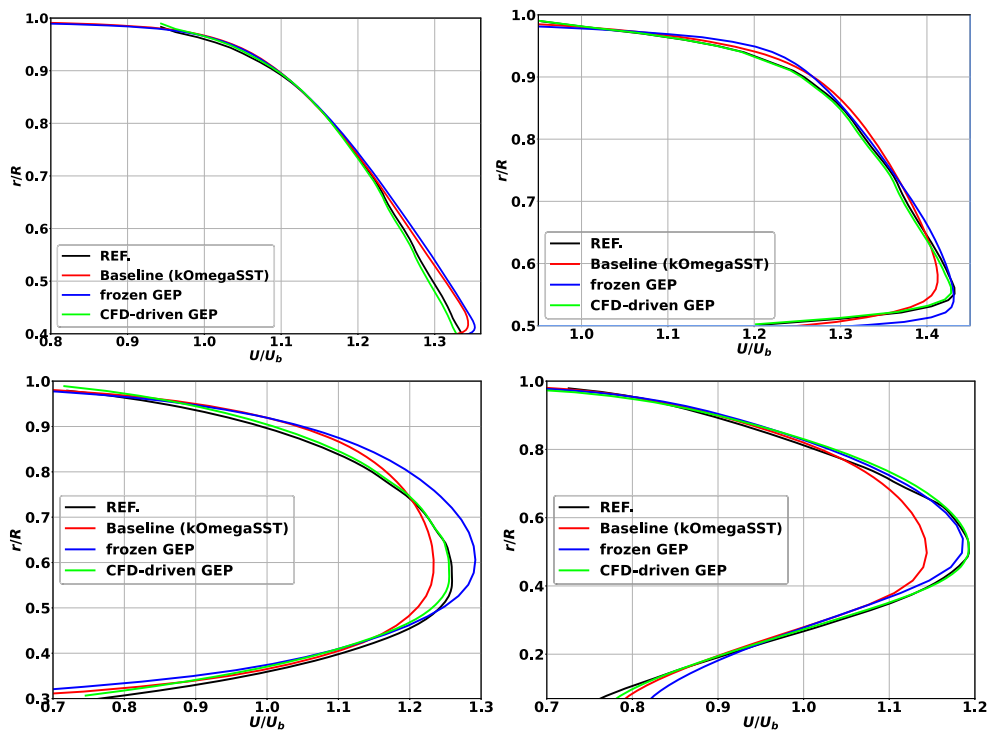


Figure 5. Comparison of experimental and numerical results in different regions for the medium body ($d/D = \sqrt{2}/3$) BOR configuration at $Re_D = 156,000$. Starting from the upper left corner figure, clockwise: x/R (BOW) = 1.1, x/R (CENTER) = 5.37, x/R (STERN) = 12.17, x/R (WAKE) = 12.9167.

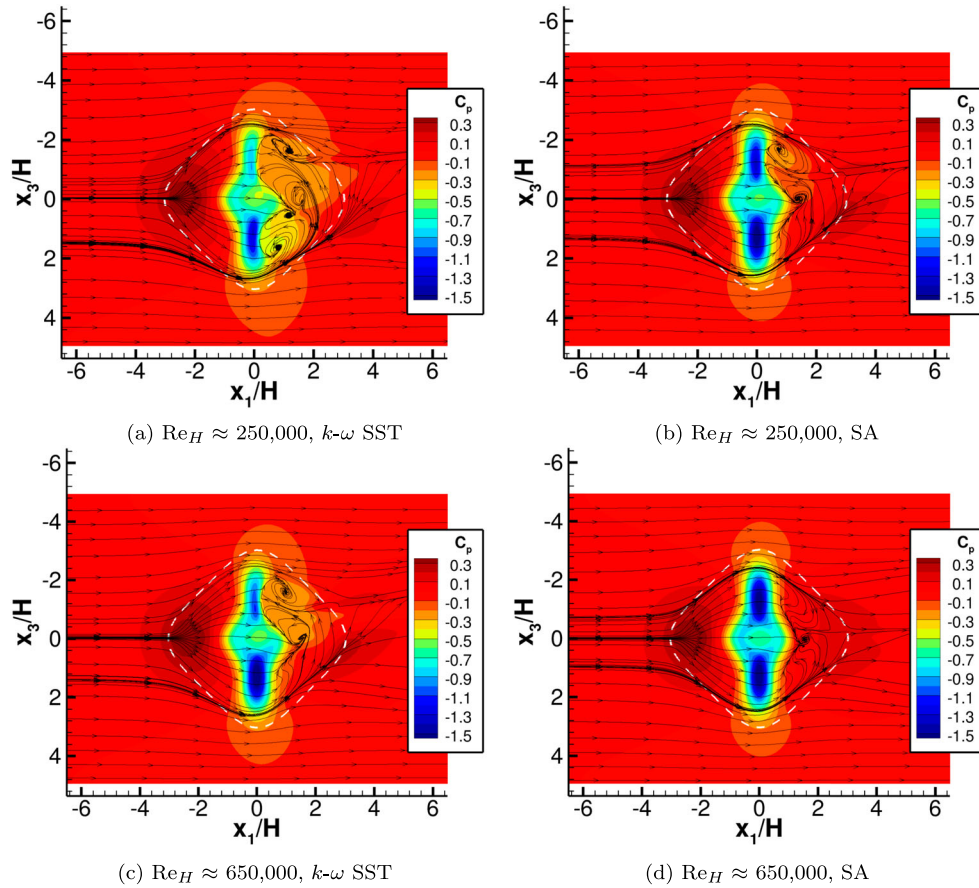


Figure 6. C_p contours with overlaid shear stress lines from the Fluent RANS simulations of the 45° yaw case BeVERLI Hill on the Level 1 grid. The perimeter of the BeVERLI Hill is represented as a white-coloured dashed line. Images extracted from Gargiulo et al. [2]. (a) $Re_H \approx 250,000$, $k-\omega$ SST. (b) $Re_H \approx 250,000$, SA. (c) $Re_H \approx 650,000$, $k-\omega$ SST and (d) $Re_H \approx 650,000$, SA.

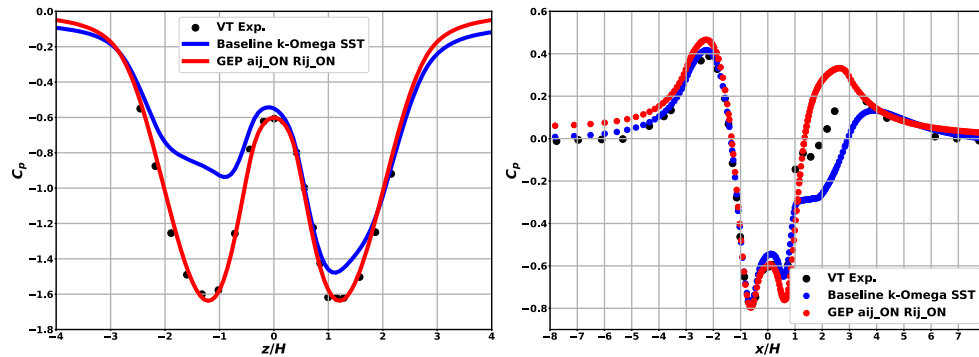


Figure 7. Cross-comparison of BeVERLI Hill surface C_p distribution along the (left) hill centerspan ($x = 0$) and (right) hill centreline ($z = 0$) planes with the VT experiment at $Re_H = 250,000$, for a 45° yaw angle orientation. All calculations performed using the simpleFOAM [44] solver. The legend indicates turbulence models used for the results plotted as lines, with further details on the gene expression programming model given in Appendices C and D.

of the flow. Duetsch-Patel et al. [20, 21] also show that combinations of three-dimensional turbulent boundary layer skewing (lateral pressure gradients) and streamwise pressure gradients offer separate challenges to physical and turbulence models. While eddy viscosity/mixing length models seem to capture the effects of skewing well enough to predict mean velocity profiles (e.g.[20]), they fail for predicting even the mean flow for the accelerating flow cases mentioned above. Further work is required to develop approaches to model the cases between the extremes of highly skewed flows and highly accelerated flows. Work is especially needed

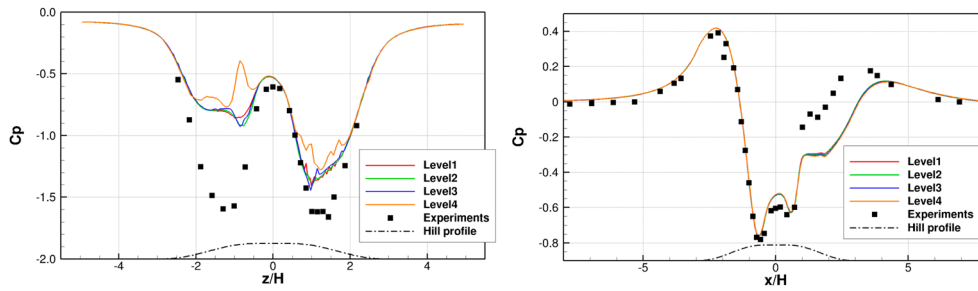


Figure 8. Pressure coefficient sensitivity to grid refinement sensitivity for results obtained using ISIS-CFD and linear isotropic $k-\omega$ SST model by Menter [9] for the 45° yaw angle orientation at $Re_H = 250,000$ along the (left) hill centerspan ($x = 0$) and (right) hill centreline ($z = 0$) planes.

to address the accrued effects of skewing and acceleration in three-dimensional boundary layers over curved surfaces.

4. Non-unique flows

Non-uniqueness, expressed by asymmetries for symmetric geometries and boundary conditions, has been observed in experiments and simulations for both the BeVERLI Hill and BB cases. With mounting evidence, it should be concluded that this occurrence is fundamental to separating flow cases.

Asymmetries in the BeVERLI Hill cases with laterally symmetric geometries (0° and 45° orientations) have been repeatedly observed in both experiments and simulations. This NATO activity enabled cross-facility studies at Virginia Tech, SINTEF Ocean, and the University of Toronto Institute for Aerospace Studies, which were pivotal in establishing facility and model independence of asymmetric and oscillating flow behaviours for the most bluff, 0° yaw case of the BeVERLI Hill. The unsteady, chaotic symmetry switching from these experiments is very different from vortical shedding phenomenon such as vortex street formation of the circular cylinder. Strouhal numbers based on the approach freestream velocity and hill height are on the order of 0.003: two orders of magnitude lower than typical shedding from cylindrical bodies. The relative rarity of switching between asymmetric mean flows empirically indicates stability of asymmetric flow solutions. This was seen in the earliest RANS solutions for the 0° case, at first as a confusing and questionable result, but now understood to be fundamental to RANS solutions for symmetric separation. The symmetry switching behaviour of the 0° case makes experiments very difficult to carry out. (e.g. A $2/3^{rd}$ s scale model was studied by UTIAS and Virginia Tech in the Stability Wind Tunnel in which the mean time between switching was approximately 4 seconds [18]. Obtaining low-error statistics for many asymmetry switches requires hours of data. This realisation also makes clear that such timescales will not be accessible for eddy resolving methods due to computational costs.) It should be noted that these observations are quite similar to those found for the Ahmed body (e.g. [45]). Given the challenges posed by the mean flow switching of the 0° case, more emphasis was placed on experiments and computations for the 45° incidence case, as discussed in detail in Appendix C. Experiments on this most streamlined of BeVERLI Hill yaw angles indicate steady mean flow that is relatively symmetric at lower Reynolds numbers ($Re_H = 250,000$ and $375,000$), developing strong asymmetry at the highest Reynolds number studied ($Re_H = 650,000$). In contrast, virtually all RANS calculations indicated asymmetric solutions, even for the low Reynolds numbers that are found to be symmetric in experiments. The gene expression programming models developed by the University of Melbourne showed that changing the turbulence model could result in symmetric solutions to better match the low Reynolds number findings.

Both the University of Washington and University of Notre Dame experiments on the BB show slight asymmetry in the spanwise surface pressure across the peak of the hill. At the very least, this shows that these flows can be quite sensitive and difficult to maintain symmetry [3, 28]. Given the asymmetric solutions seen on the BeVERLI Hill, the University of Washington team were interested to look at side-to-side motions in the wake of the BB to compare and to contrast. Both top-down PIV and high-rate pressure measurements were acquired in the wake of the BB revealing a strong side-to-side motion at low frequency (roughly comparable to BeVERLI Hill) [26]. Interestingly, this motion is seen to have a probability density function that is single peaked, suggesting that it is more of a continuously varying motion than observed for the BeVERLI Hill and that

the BB does not exhibit a bi-stable solution, despite frequency similarity to the BeVERLI Hill. Analysis of the connections between this spanwise motion and the streamwise modes seen at the centreline is ongoing. Asymmetric simulation solutions have also been observed for the BB. Williams et al. [3] showed that refinement of the simulations removed asymmetries that were initially observed. Gray et al. [28] observed asymmetric solutions for SST-quadratic constitutive relation (QCR) simulations at some higher Reynolds numbers. Gray et al. [24] also saw asymmetries for some delayed-detached eddy simulation (DDES) computations. Finally, Shur et al. [37] note unpublished simulations from their group and Sandia National Laboratories that have observed asymmetric solutions using RANS that are resolution and model dependent.

The fundamental nature of asymmetry in separating flow cases presents several important challenges for improving computations and models for engineering-relevant, three-dimensional geometries. First, it must be recognised that three-dimensional flow geometries, even those with two-dimensional (cylindrical) sections, cannot be accurately captured with a two-dimensional conceptual or computation model. As with the relaminization topic above, this statement requires nuance in interpreting, as there is a spectrum of influence from the effects of asymmetry, with the BB being less influenced due to its wider aspect ratio compared to the greater influence seen on the BeVERLI Hill cases. A second challenge is in understanding local discrepancies seen between computational solutions and experimental results when multiple solutions exist. In these cases, especially as seen for the computations on the BeVERLI hill, when multiple solutions exist, the effects of modelling are inseparable from the propensity of the solver and the equations solved to prefer one solution over another. These solutions may (and likely do) have relationships to physical reality for the boundary conditions, but comparing these when a different solution is realised from experiments is impossible.

Engineers and designers need practical approaches for assessing geometries and flows which result in multiple solutions. Of high value would be the ability to anticipate the presence of chaotic unsteadiness, such as seen with the 0° incidence BeVERLI Hill geometry. Best practices need to be developed for analysing unsteady forces for these cases. At a minimum, running long duration unsteady solutions could provide insight for cases anticipated to present issues, although it is unknown which framework is best to use among unsteady RANS, detached eddy simulation, WMLES, or wall-resolved LES. Given the great impact on system integrity and vehicle control, this is a pressing and first-order need for a designer. Furthermore, there are cases of inherent mean flow asymmetry for laterally symmetric boundary conditions that appear to lack global-scale unsteadiness. As of now it appears, but is not proven, that asymmetric solutions obtained by RANS are topologically indicative of modes of asymmetric solutions. Further work is needed to address scientific and engineering-relevant questions on how best to conduct and use simulations in cases of both steady and unsteady multi-solution flow fields.

5. Other common features

The asymmetric solutions just discussed provide examples of a key challenge facing the ability to gain insights from experimental and computational results comparisons. However, the activity revealed additional issues that beg discussions. Notably, the handling of the inflow profile development of the Princeton BOR case required special attention beyond the simple specification of an inflow profile. It was seen that the fully developed pipe flow streamwise mean velocity profile computed using several RANS models deviated significantly from the experimentally observed profile in the wake region as the flow approached the BOR. The flow solutions over the body were sensitive to this effect and required normalisation by the centreline velocity approaching the BOR for a better comparison. The boundary layer flow over the BeVERLI Hill was apparently less affected by this, but guess-and-check effort was still required to specify the entrance domain for matching boundary layer parameters at the reference plane in the experimental flow.

The SSG-LRR Reynolds stress transport model was shown to improve the prediction in the bow region of the Princeton BOR case compared with the 2003 Menter $k-\omega$ SST eddy viscosity model. For both the Princeton BOR and the BeVERLI Hill cases, models built using gene expression programming showed promise in improving simulation results in attached flow regions.

One of the challenges to using Reynolds stress transport modelling is maintaining the stability of solutions at higher Reynolds numbers. There are opportunities and needs for developing numerical treatments to support implementation of these models.

Some of the effects that were identified as problematic in this activity (particularly relaminarization) will be reduced in importance at the very high Reynolds numbers of many industrially relevant vehicles. There is a general need to provide test cases and experimental results for very high Reynolds number flows, particularly containing key complications such as convolved effects of pressure gradient and curvature.

6. Conclusions

A concerted activity involving highly integrated computations and experiments has been completed to assess and advance the status of predictions and understanding for flows over axisymmetric and three-dimensional bodies. The cases considered for the current study were an axisymmetric body-of-revolution immersed in a fully developed pipe flow, and two different cases involving boundary layer flows which encounter three-dimensional hill geometries. The Princeton BOR flow offered a case which contained curvature effects and included accentuated effects from forebody acceleration and boundary layer recovery in a nearly constant pressure gradient region. The BeVERLI Hill offers a highly three-dimensional geometry that exhibits a range of steady and unsteady global topological and flow features dependent upon the orientation of the hill relative to the approaching boundary layer flow. Computations specific to the current activity were conducted for both these cases. A third case based upon a thin turbulent boundary layer flowing over a Gaussian bump, termed the Boeing Speed-Bump in the current context, was further analysed based upon experimental results from the present activity and computational results gleaned from the literature. The BB has a higher lateral aspect ratio than the BeVERLI Hill and, thus, weaker three-dimensionality. All cases studied exhibit high windward flow acceleration, while both of the hill cases also exhibit flow separation. The separating cases exhibit some degree of mean flow lateral asymmetry despite having laterally symmetric geometries. Further, the 0° incidence BeVERLI Hill case shows very low frequency, unsteady asymmetry switching.

The activity resulted in several important findings that can guide studies and practice for computing the flow over three-dimensional bodies:

- Accelerating flow regions present major challenges to the accuracy of computations due to shortcomings in RANS turbulence models. The rapid distortion of turbulence is not properly captured by eddy viscosity models, resulting in more modelled turbulent stress than is seen in reality. Although this effect is Reynolds number dependent, it is an observation shared for each of the flow cases considered. It was shown for the BOR case that Reynolds stress transport modelling (SSG-LRR) could improve predictions in the highly accelerated region, likely due to improved predictions of rapid distortion on turbulence anisotropy and magnitudes. However, this model was not as effective as a linear eddy viscosity model (2003 Menter $k-\omega$ SST) in regions downstream of the bow. Solutions of the BeVERLI Hill at 45° incidence are sensitive to choice of eddy viscosity turbulence models (Spalart Allmaras versus 2003 Menter $k-\omega$ SST) in the region just downstream of windward acceleration. Gene expression programming, in which experimental data are used to generate optimised constitutive relations and modified turbulence production, showed promise for improving the flow solutions in accelerated flow regions for the BOR and BeVERLI Hill cases.
- The combined effects of streamwise curvature and pressure gradient are also universally present in the cases studied, and these effects are likely a cause of modelling discrepancy in attached flow regions. There remains the need for comprehensive RANS-based modelling approaches that can properly capture these combined effects. Furthermore, the difficulty in separating the contributions from pressure gradient versus curvature to turbulence transport has led to few fundamental insights in the literature or from current results. Further and creative approaches are needed to better assess these combined complications.
- The fully developed pipe inflow of the BOR case exposed challenges in matching inflow profiles. The results for flow over the body were sensitive to this effect, indicating the need to carefully handle inflow conditions for validation cases based upon fully developed inflow conditions.
- There is ample evidence to state that non-unique and asymmetric global flow solutions are fundamental to flow cases with lateral geometric symmetry involving turbulent boundary layer separation. An important feature of the current study was the ability to rule out facility- or hardware-specific causes for

asymmetry, as results were replicated at multiple facilities and using different experimental model hardware. The current studies have established that laterally symmetric grids can produce laterally asymmetric flow field solutions. Furthermore, there are some asymmetric flow fields that are unsteady (exhibiting asymmetry switching) and others that are steadily asymmetric. These features cause difficulties in comparing computational solutions to experimental results and even in comparing computational results across different turbulence models or solvers (even for the same grid). It still remains to be determined whether the asymmetric solutions obtained by RANS are equivalent or approximately equivalent to asymmetric modes observed in experiments with unsteady switching. Despite the challenges, configurations of engineering relevance exist for geometries that yield such behaviours and which require analysis of loads. Additional fundamental work is needed to fully develop the understanding of the global flow physics leading to these observations. With this understanding, a valuable contribution would be the development of engineering tools that can predict the presence and magnitude of global unsteadiness that will lead to undesirable loads for configurations in early design phases.

- The cases studied are at lower Reynolds numbers than seen for most full-scale vehicles. While the parameter space for high Reynolds number applications may ultimately show reduced importance of acceleration and curvature effects, non-unique flow solutions are likely to remain. Furthermore, observations regarding the relative importance of pressure gradient, curvature, and mean flow meandering will continue to pose issues for contemporary RANS methods and turbulence models. Creative approaches to supplementing the knowledge of three-dimensional flow cases at very high Reynolds numbers are needed for advancing the capability and confidence of modelling methods in this regime.

Acknowledgments

The compilation of this chapter included contributions from a number of other collaborators on NATO activity AVT-349. Their many contributions are gratefully acknowledged.









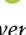

Disclosure statement

No potential conflict of interest was reported by the author(s).

Funding

The experimental work for the Body of Revolution Case was supported by ONR under Grant N00014-17-1-2309 (Program Manager Peter Chang). The experimental work for the Virginia Tech efforts on the BeVERLI hill case was funded by National Aeronautics and Space Administration (NASA) (Grant Nos. 80NSSC18M0146 and 80NSSC22M0061) (Program Monitors Michael Kegerise and Mujeeb Malik). The work performed by the ECN/CNRS authors was granted access to the HPC resources made available by GENCI (Grant-A0082A00129, Grant-A0102A00129). The work performed at the University of Melbourne was funded by the Australian Research Council and U.S. Office of Naval Research (ONR) under NICOP Grant N62909-20-1-2046 with program monitors Elena McCarthy (ONR-G), Yin Lu (Julie) Young (ONR). The research by MARIN is partly funded by the Dutch Ministry of Economic Affairs.

ORCID

Todd Lowe  <http://orcid.org/0000-0002-0147-4641>
Alexander J. Smits  <http://orcid.org/0000-0002-3883-8648>
Michel Visonneau  <http://orcid.org/0000-0003-1676-5326>
Ganbo Deng  <http://orcid.org/0000-0001-9794-7687>
Emmanuel Guilmineau  <http://orcid.org/0000-0001-9070-093X>
Richard Sandberg  <http://orcid.org/0000-0001-5199-3944>
Julie Duetsch-Patel  <http://orcid.org/0000-0001-8480-9891>
Philippe Lavoie  <http://orcid.org/0000-0002-7233-1779>
Luca Savio  <http://orcid.org/0000-0001-6387-2576>
William Devenport  <http://orcid.org/0000-0002-3413-861X>

References

- [1] Ding L, Saxton-Fox T, Hultmark M, et al. Effects of pressure gradient and streamline curvature on the statistics of a turbulent pipe flow. In: Proc. Turbulence and Shear Flow Phenomena 11. University of Southampton, Southampton, UK; 2019. p. 353.
- [2] Gargiulo A, Duetsch-Patel JE, Borgoltz A, et al. Strategies for computational fluid dynamics validation experiments. *J Verif Valid Uncert Quantif*. 8(3). 2023. Accepted Manuscript. doi: [10.1115/1.4063639](https://doi.org/10.1115/1.4063639).
- [3] Williams O, Samuell M, Sarwas ES, et al. Experimental study of a CFD validation test case for turbulent separated flows. In: AIAA Scitech 2020 Forum; 2020. p. 0092.
- [4] Moonesun M, Korol YM, Dalayeli H, et al. Optimization on submarine stern design. *Proc Inst Mech Eng Part M J Eng Marit Environ*. 2017;231(1):109–119.
- [5] Visonneau M, Guilmineau E, Deng G, et al. Bodies-of-revolution in turbulent flow: comparing computation with experiment. *AIAA Paper 22-0694*. 2022.
- [6] McKeon BJ, Swanson CJ, Zagarola MV, et al. Friction factors for smooth pipe flow. *J Fluid Mech*. 2004;511:41–44. doi: [10.1017/S0022112004009796](https://doi.org/10.1017/S0022112004009796)
- [7] Menter FR. Two-equation eddy-viscosity turbulence models for engineering applications. *AIAA J*. 1994;32(8):1598–1605. doi: [10.2514/3.12149](https://doi.org/10.2514/3.12149)
- [8] Cécora RD, Radespiel R, Eisfeld B, et al. Differential reynolds-stress modeling for aeronautics. *AIAA J*. 2015;53(3):1–17. Published online: 10 September 2014, March 2015.
- [9] Menter FR, Kuntz M, Langtry R, et al. Ten years of industrial experience with the sst turbulence model. *Turbul Heat Mass Transf*. 2003;4(1):625–632.
- [10] Rumsey C. Nasa langley research center turbulence modeling resource. NASA Langley Research Center, Hampton, VA. 2017; https://turbmodels.larc.nasa.gov/nasahump_val_sa.html [retrieved Sept. 2016]. [Google Scholar].
- [11] Weatheritt J, Sandberg R. A novel evolutionary algorithm applied to algebraic modifications of the rans stress–strain relationship. *J Comput Phys*. 2016;325:22–37. doi: [10.1016/j.jcp.2016.08.015](https://doi.org/10.1016/j.jcp.2016.08.015)
- [12] Zhao Y, Akolekar HD, Weatheritt J, et al. RANS turbulence model development using CFD-driven machine learning. *J Comput Phys*. 2020;411:109413. doi: [10.1016/j.jcp.2020.109413](https://doi.org/10.1016/j.jcp.2020.109413)
- [13] Waschkowski F, Zhao Y, Sandberg R, et al. Multi-Objective CFD-driven development of coupled turbulence closure models. *J Comput Phys*. 2022;452:110922. doi: [10.1016/j.jcp.2021.110922](https://doi.org/10.1016/j.jcp.2021.110922)
- [14] Schmelzer M, Dwight RP, Cinnella P. Discovery of algebraic reynolds-stress models using sparse symbolic regression. *Flow Turbul Combust*. 2020;104:579–603. doi: [10.1007/s10494-019-00089-x](https://doi.org/10.1007/s10494-019-00089-x)
- [15] Gargiulo A, Beardsley C, Vishwanathan V, et al. Examination of flow sensitivities in turbulence model validation experiments. In: AIAA Scitech 2020 Forum; Jan. American Institute of Aeronautics and Astronautics; 2020. p. 1–23. doi: [10.2514/6.2020-1583](https://doi.org/10.2514/6.2020-1583).
- [16] Duetsch-Patel JE, Gargiulo A, Borgoltz A, et al. Structural aspects of the attached turbulent boundary layer flow over a hill. *Exp Fluids*. 2023;64(2):38. doi: [10.1007/s00348-023-03580-4](https://doi.org/10.1007/s00348-023-03580-4)
- [17] Duetsch-Patel JE, MacGregor D, Jenssen YL, et al. The BeVERLI hill three-dimensional separating flow case: cross-facility comparisons of validation experiment results. In: AIAA Scitech 2022 Forum; January. American Institute of Aeronautics and Astronautics; 2022. p. 1–22. doi: [10.2514/6.2022-0698](https://doi.org/10.2514/6.2022-0698).
- [18] MacGregor DA, Gargiulo A, Duetsch-Patel JE, et al. Mean and unsteady surface-pressure measurements on the beverli hill. In: AIAA SciTech 2023 Forum; National Harbor, MD, USA and Virtual; 2023. AIAA Paper 2023–0468.
- [19] Gargiulo A. Direct assessment and investigation of nonlinear and nonlocal turbulent constitutive relations in three-dimensional boundary layer flow [dissertation]. Virginia Tech; 2023.
- [20] Duetsch-Patel JE, Gargiulo A, Borgoltz A, et al. Boundary layer flow over a bump and the three-dimensional law of the wall. *J Turbul*. 2023;24(3-4):2202404. doi: [10.1080/14685248.2023.2202404](https://doi.org/10.1080/14685248.2023.2202404)
- [21] Duetsch-Patel JE. Structure and turbulence of the three-dimensional boundary layer flow over a hill [dissertation]. Virginia Tech; 2023.
- [22] Sundarraj V, MacGregor DA, Gargiulo A, et al. Estimation of skin friction on the nasa beverli hill using oil film interferometry. In: AIAA Scitech 2023 Forum; 2023. AIAA 2023–0988.
- [23] Lowe T, Borgoltz A, Devenport WJ, et al. Status of the NASA/Virginia tech benchmark experiments for CFD validation. In: AIAA SciTech 2020 Forum; 1; Orlando; 2020. p. 2020–1584.
- [24] Gray PD, Lakebrink MT, Thomas FO, et al. Experimental and computational evaluation of smooth-body separated flow over boeing bump. In: AIAA AVIATION 2023 Forum; 2023. p. 3981.
- [25] Williams OJ, Annamalai H, Ozoroski TA, et al. Comparison of hill-type geometries for the validation and advancement of turbulence models. In: AIAA SCITECH 2022 Forum; 2022. p. 1032.
- [26] Manohar KH. Sensor-based temporal superresolution: Application to turbulent separated flow over a three-dimensional Gaussian hill [master’s thesis]. University of Calgary; 2023.
- [27] Williams OJ, Samuell M, Robbins ML, et al. Characterization of separated flowfield over gaussian speed-bump cfd validation geometry. In: AIAA Scitech 2021 Forum; 2021. p. 1671.
- [28] Gray PD, Gluzman I, Thomas F, et al. A new validation experiment for smooth-body separation. In: AIAA Aviation 2021 Forum; 2021. p. 2810.

- [29] Robbins M, Samuell M, Williams OJ. Uncertainty quantification of a Gaussian speed bump separated flow validation test case. In: SciTech Forum; 2021.
- [30] Balin R, Jansen KE, Spalart PR. Wall-modeled les of flow over a gaussian bump with strong pressure gradients and separation. In: AIAA Aviation 2020 Forum; 2020. p. 3012.
- [31] Agrawal R, Whitmore MP, Griffin KP, et al. Non-boussinesq subgrid-scale model with dynamic tensorial coefficients. *Phys Rev Fluids*. 2022;7(7):074602. doi: [10.1103/PhysRevFluids.7.074602](https://doi.org/10.1103/PhysRevFluids.7.074602)
- [32] Iyer PS, Malik MR. Wall-modeled les of flow over a gaussian bump. In: AIAA Scitech 2021 Forum; 2021. p. 1438.
- [33] Wright JR, Balin R, Jansen KE, et al. Unstructured les_dns of a turbulent boundary layer over a gaussian bump. In: AIAA Scitech 2021 Forum; 2021. p. 1746.
- [34] Rizzetta DP, Garmann DJ. Wall-resolved large-eddy simulation of flow over a parametric set of gaussian bumps. In: AIAA AVIATION 2023 Forum; 2023. p. 3983.
- [35] Uzun A, Malik MR. Simulation of a turbulent flow subjected to favorable and adverse pressure gradients. *Theor Comput Fluid Dyn*. 2021;35:293–329. doi: [10.1007/s00162-020-00558-4](https://doi.org/10.1007/s00162-020-00558-4)
- [36] Uzun A, Malik MR. High-fidelity simulation of turbulent flow past gaussian bump. *AIAA J*. 2022;60(4):2130–2149. doi: [10.2514/1.J060760](https://doi.org/10.2514/1.J060760)
- [37] Shur ML, Spalart PR, Strelets MK, et al. Direct numerical simulation of the two-dimensional speed bump flow at increasing reynolds numbers. *Int J Heat Fluid Flow*. 2021;90:108840. doi: [10.1016/j.ijheatfluidflow.2021.108840](https://doi.org/10.1016/j.ijheatfluidflow.2021.108840)
- [38] Gargiulo A, Duetsch-Patel JE, Ozoroski TA, et al. Flow field features of the BEVERLI hill model. In: AIAA Scitech 2021 Forum; 2021. p. 1741.
- [39] Lowe T, Roy CJ, Devenport WJ, et al. Experimental results for the VT-NASA CFD turbulence model blind validation challenge. In: AIAA Aviation Forum and Ascend 2024; 2024. AIAA 2024–4438.
- [40] Roy CJ, Lowe T, Devenport WJ, et al. Summary of data from the VT-NASA blind validation CFD challenge case. In: AIAA Aviation Forum and Ascend 2024; 2024. AIAA 2024–4439.
- [41] Roy CJ, Lowe T, Devenport WJ, et al. A blind validation CFD challenge case for 3D smooth-body turbulent separation. In: AIAA Aviation 2023 Forum; 2023. p. 3986.
- [42] Devenport WJ, Lowe KT. Equilibrium and non-equilibrium turbulent boundary layers. *Prog Aerosp Sci*. 2022;131:100807. doi: [10.1016/j.paerosci.2022.100807](https://doi.org/10.1016/j.paerosci.2022.100807)
- [43] Shur ML, Spalart PR, Strelets MK, et al. A hybrid rans-les approach with delayed-des and wall-modelled les capabilities. *Int J Heat Fluid Flow*. 2008;29(6):1638–1649. doi: [10.1016/j.ijheatfluidflow.2008.07.001](https://doi.org/10.1016/j.ijheatfluidflow.2008.07.001)
- [44] Weller HG, Tabor G, Jasak H, et al. A tensorial approach to computational continuum mechanics using object-oriented techniques. *Comput Phys*. 1998;12(6):620–631. doi: [10.1063/1.168744](https://doi.org/10.1063/1.168744)
- [45] Grandemange M, Gohlke M, Cadot O. Turbulent wake past a three-dimensional blunt body. Part 1. Global modes and bi-stability. *J Fluid Mech*. 2013;722:51–84. doi: [10.1017/jfm.2013.83](https://doi.org/10.1017/jfm.2013.83)